

ARTICLE

Supporting Information

The Location of Metastasis Lymph Node and the Evaluation of Lymphadenectomy by Near-infrared Photoacoustic Imaging with Iridium Complexes Nanoparticles

Qi Yang,^{*a} Yajun Yu,^{*a} Chaojie Tang,^b Yucong Gao,^a Wu Wang,^{*b} Zhiguo Zhou,^a Shiping Yang,^a Hong Yang,^{*a}

Model	4T1
Start time	10:02
Injection time	10:09
Residual time	10:14
Original amount (μG)	102
Residual amount (μG)	5
Body weight	21.7
SUV	4.6

Table S1. The injection amount of ¹⁸F-FDG for tumor mice.

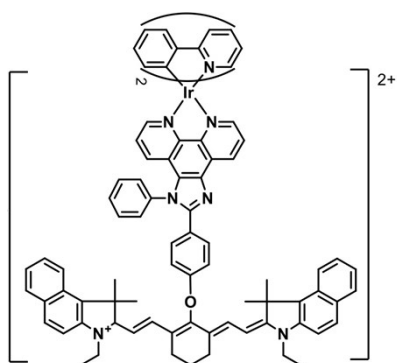


Fig. S1† The chemical structure of IrCy.

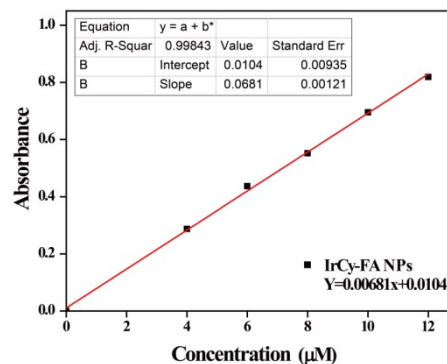


Fig. S2† The standard calibration curve of IrCy-FA NPs calculated from ICP quantitative data of Ir.

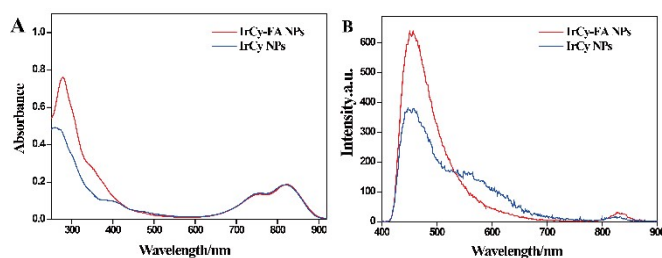


Fig. S3† (A) The absorbance of IrCy-FA NPs (red) and IrCy NPs (blue). (B) The fluorescence intensity of IrCy-FA NPs (red) and IrCy NPs (blue). Note, IrCy NPs was a control material, can be considered as without modifying folic acid to IrCy-FA NPs surface.

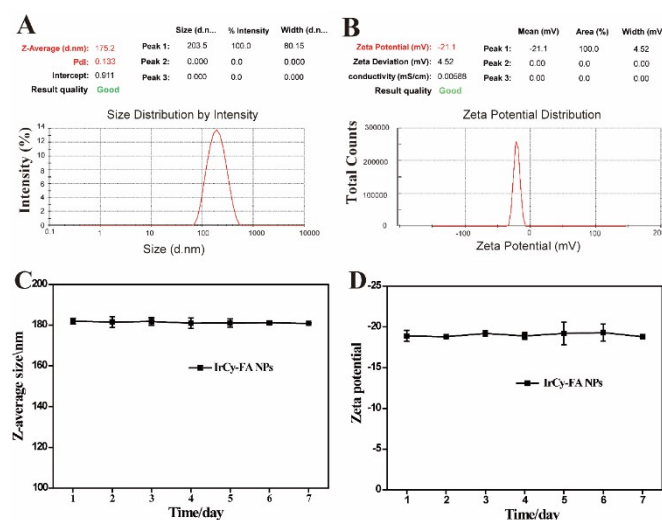


Fig. S4† (A) The hydrodynamic diameter of IrCy-FA NPs in an aqueous

solution. (B) The Zeta Potential of IrCy-FA NPs in an aqueous solution. (C) The time-dependent hydrodynamic diameter of IrCy-FA NPs in PBS at 25 °C. (D) The time-dependent Zeta potential of IrCy-FA NPs in PBS at 25 °C.

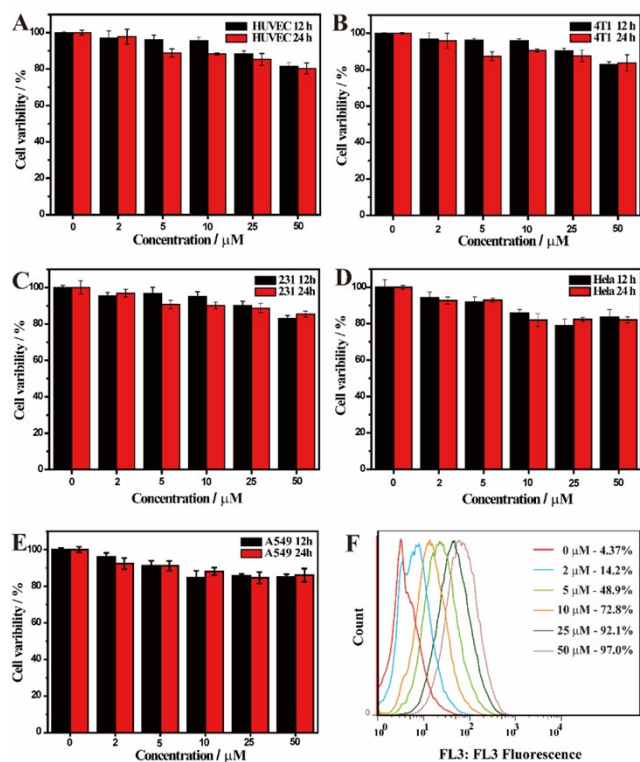


Fig. S5† The cell viability for tumor cells that cultured with different concentrations of IrCy-FA NPs (0, 2, 5, 10, 25, and 50 μM , respectively). (A) HUVEC cells, (B) 4T1 cells, (C) MDA-MB-231 cells, (D) HeLa cells, (E) A549 cells. (F) The flow cytometry analysis for 4T1 cells uptake efficiency of IrCy-FA NPs with different incubated concentrations (0, 2, 5, 10, 25, and 50 μM , respectively), $\lambda_{\text{ex}} = 488 \text{ nm}$.

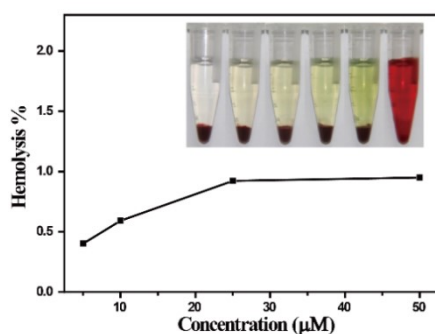


Fig. S6† The hemolysis and photographs (inset) of IrCy-FA NPs with different incubation concentrations. (0, 5, 10, 25, 50 μM in PBS solution and 0 μM in water).

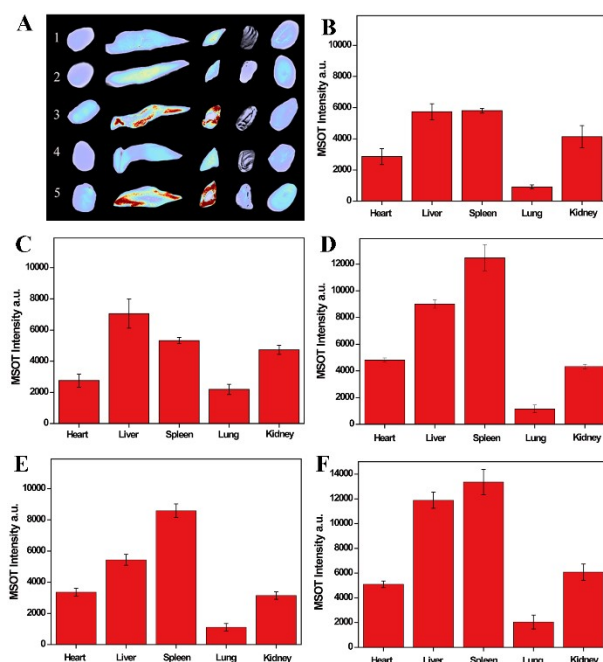


Fig. S7† The study of biodistribution of IrCy-FA NPs by PA imaging. (A) The *in vitro* PA images of dissected heart, liver, spleen, lung and kidney in five group of mice, including 1) blank mice; 2) HeLa mice, palm injection; 4) MDA-MB-231 mice, palm injection; 3) HeLa mice, tail vein injection; 5) MDA-MB-231 mice, tail vein injection. The organs are extracted after injection of IrCy-FA NPs nanoparticles for 24 h, and we used two injection methods, the palm injection and tail vein injection. Quantitative analysis of PA intensity in different injection methods: B) blank mice; (C) HeLa mice with palm injection; (D) MDA-MB-231 mice with palm injection; (E) HeLa mice with tail vein injection; (F) MDA-MB-231 mice with tail vein injection, $***p < 0.001$. Note: Injection concentrations of IrCy-FA NPs: palm injection, 1mg/mL, 20 μL ; tail vein injection, 2 mg/mL, 200 μL .

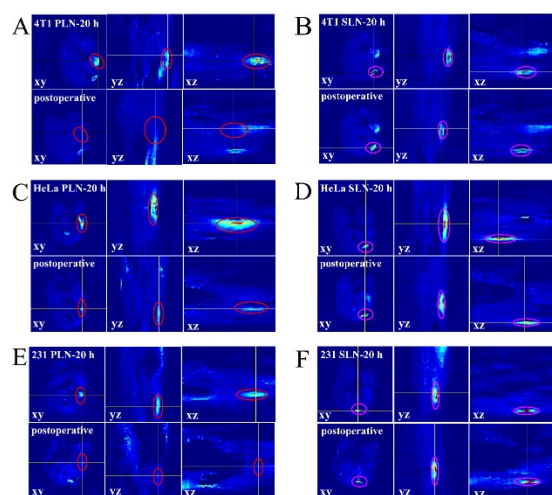


Fig. S8† The three-dimensional co-localization PA images of PLN and SLN which collected at pre- and postoperative of different tumor model lymphadenectomy (red circle, PLN; green circle, SLN). 4T1 metastasis lymph nodes model: (A) PLN and (B) SLN; HeLa metastasis lymph nodes model: (C) PLN and (D) SLN; MDA-MB-231 metastasis lymph nodes model: (E) PLN and (F) SLN.